COMPARISON OF OPTICAL AND X-RAY MASS ESTIMATES OF THE CHANDRA GALAXY CLUSTERS AT $Z < 0.1$

Iu.V. Babyk[1,2,3], I.B. Vavilova[1]

[1] Main Astronomical Observatory of NAS of Ukraine, Kyiv, Ukraine
[2] Dublin Institute for Advanced Studies, Dublin, Ireland
[3] Dublin City University, Dublin, Ireland,
babikyura@gmail.com, irivav@mao.kiev.ua

ABSTRACT. We used the optical data taken from SDSS DR7 galaxy and group catalog to determine the optical mass of 37 nearer Chandra galaxy clusters for comparison with the X-ray mass estimates. Using the assumption that mass follows the galaxy distribution, we computed the mass of each cluster by applying the virial theorem to the member galaxies. We have found a good agreement between optical and X-ray mass estimates and confirm that about 70 % of nearby galaxy clusters are not far from dynamical equilibrium.

Key words: Galaxy clusters: optical mass of galaxy clusters.

1. Introduction

The knowledge of the main characteristics of galaxy clusters plays a significant role in the study of the large-scale structure of the Universe. Among these characteristics the correct mass estimates are important for understanding both the intrinsic visible/dark matter distribution in clusters and evolution processes at the cosmological scales. The classical method of cluster mass calculation is the virial theorem to positions and velocities of cluster member galaxies. Another recent methods are based on the dynamical analysis of X-ray gas in clusters, and on the gravitational lensing of background galaxies etc.

Mass estimates obtained from the dynamical analysis of gas or cluster member galaxies based on the virial theorem assume that clusters are the systems in dynamical equilibrium. This assumption is not strictly valid; in fact, although clusters are the gravitationally bound galaxy systems, they collapsed recently in the cosmological sense or are being collapsed, which is confirmed by the observed frequent presence of substructures. Nevertheless, the estimate of optical virial mass still remains robust even with the presence of small substructures in galaxy clusters.

In this paper we use the SDSS DR7 group catalogs by Yang et al. (2007), which are constructed from the SDSS spectroscopic data. These catalogs provide us with galaxy clusters that have reliable galaxy memberships, which are important in probing the halo occupation distribution statistics and galaxy formation models. The SDSS DR7 group catalogs also span a large halo mass range, from rich clusters to the isolated faint galaxies, allowing us to investigate the X-ray luminosity and hot gas distribution not only in massive clusters but also in relatively small halos.

The aim of this work is to obtain the optical mass estimates of 37 nearer Chandra galaxy clusters for comparison with the X-ray mass estimates obtained in our previous works (Babyk et al. 2012a,b,c,d). The paper is organized as follows. We describe briefly the data sample and selection procedure for cluster membership assignment in Section 2. We explain the methods to compute the masses of clusters using member galaxies in Section 3 and discuss our results in Section 4. We used the cosmological parameters $H_0 = 73$ km/s/Mpc, $\Omega_M = 0.27$, and $\Omega_\Lambda = 0.73$.

2. The optical data collection

We collected the optical data for 37 nearer Chandra galaxy clusters at $0.01 < z < 0.1$ using literature and databases. We considered the clusters for which Yang et al. (2007) gave an estimate for the velocity dispersion using the optical data from SDSS galaxy group catalogs. It was compiled with the adaptive halo-based group finder by Yang et al. (2005) and then updated to SDSS DR7. They select all galaxies in the Main Galaxy Sample with an extinction-corrected apparent magnitude brighter than 17.72, with redshifts in the range $0.01 < z < 0.20$ and with a redshift completeness $C_z > 0.7$. The resulting SDSS galaxy catalog contains a total of 639359 galaxies, with a sky coverage of 7748 square degrees. It is important to note that a very small fraction of galaxies in this catalog have redshifts taken from the Korea Institute for Advanced Study (KIAS) Value Added Galaxy Catalog (VAGC) (e.g. Choi et al. 2010).

3. Determination of the mass of clusters from the Virial theorem

3.1. Theoretical approach

One of the best way to estimate the mass of clusters from member galaxies requires that galaxies should be in the equilibrium with a cluster potential. As result, the cluster mass can be found from positions and velocities of the same population of galaxies. We describe below the main steps which were applied to compute the masses of galaxy clusters from the virial theorem.

The virial mass of clusters, M_{vir}, depends from the spatial distribution of the galaxy population and the global velocity dispersion, σ, as

$$M_{vir} = \frac{< v^2 >}{G < r^{-1} F >} \quad (1)$$

where r is the distance from center of cluster, v is the galaxy velocity, and F is the mass fraction within r. Then, if equation $\rho_{mass} \propto \rho$ is correct (i.e. that mass is distributed as in the observed galaxies) we can rewrite Eq. (1), as

$$M_{vir} = \frac{2 < v^2 >}{G < r_{ij}^{-1} >} = \frac{\sigma^2 R_{vir}}{G}, \quad (2)$$

where R_{vir} is the virial radius, which depends on the distance between any pair of galaxies r_{ij}. Because of the velocity dispersion and consequently the total mass is independent on any possible anisotropy of galaxy velocities, we can rewrite the Eq. (2) in the case of spherical galaxy systems for the projected quantities σ_P and R_{PV} as

$$M_{vir} = \frac{3\pi}{2} \frac{2 < V^2 >}{G < R_{ij}^{-1} >} = \frac{3\pi}{2} \frac{\sigma_P^2 R_{PV}}{G}, \quad (3)$$

In our work, the projected virial radius, R_{PV}, and velocity dispersion, σ_P, are derived as

$$\sigma_P = \sqrt{\frac{\sum_i V_i^2}{N-1}}, \quad (4)$$

$$R_{PV} = \frac{N(N-1)}{\sum_{i>j} R_{ij}^{-1}}. \quad (5)$$

3.2. Measurements

Using assumption that the number galaxies distribution traces the mass distribution we can calculate the masses of cluster by the virial theorem. We can determine the observational dispersion profile $\sigma_P(R)$ combining the data from many clusters because of such profile requires a huge amount of members (galaxies). To estimate the values of projected velocity dispersions, σ_P, we used the procedure suggested by Fadda et al. (1996). It is significant to note again that the virial theorem is reliable if the galaxy system is in the dynamical equilibrium within the considered region. As result, we are able to determine the masses of clusters within the some radius of virialization, R_{virial}. To determine this radius we applied the methods suggested by Girardi et al.(1995, 1998). In this way, the virial mass ($M_{vir} = 4\pi R_{virial}^3 \rho_{virial}/3$) can be found as $(3\pi/2)(\sigma_P^2 R_{PV}/G)$ (see Eq. (3)). As result,

$$R_{virial}^3 = \frac{\sigma_P R_{PV}}{6\pi H_0^2}, \quad (6)$$

where R_{PV} is the projected virial radius. Girardi et al. (1995) showed that R_{PV} is related to the radius of the sampled region, i.e. the aperture A (here equal to R_{virial}) as

$$R_{PV} = 1.193 A \frac{1 + 0.032(A/R_c)}{1 + 0.107(A/R_c)}, \quad (7)$$

here R_c is the core radius, which is equal to 0.17 h^{-1} Mpc. Using Eq. (6) and (7) we can find relation between R_{virial} and σ_P, as

$$R_{virial} \sim 0.002 \sigma_P (h^{-1} Mpc), \quad (8)$$

here σ_P is given in km s^{-1}.

We extract the galaxy distribution of 37 studied clusters with at least ten galaxies up to R_{virial}. The galaxy distribution inside these clusters was analyzed by the method suggested by Girardi et al. (1995), where the galaxy surface density was approximated by King profile with a variable exponent

$$\sum(R) = \frac{\sum_0}{[1 + (R/R_c)^2]^\alpha}, \quad (9)$$

where α is the value which describes the galaxy distribution (usually equal 1). Using Eq. (9), we can calculate the surface density in the following way $\rho = \frac{\rho_0}{[1+(r/R_c)^2]^{3\beta_{fit,gal}/2}}$, where $\beta_{fit,gal} = (2\alpha + 1)/3$, as result, $\rho(r) \propto r^{-3\beta_{fit,gal}}$ when $r >> R_c$. We have used likelihood technique to perform our fit. We varied α and R_c from 0.5 to 1.5 and 0.01 to 1, respectively, and verifying fitted profiles using χ^2-test. We found that $\alpha = 0.70^{+0.08}_{-0.04}$ for 2σ confidence level, as result, $\beta_{fit,gal} = 0.8$, i.e. $\rho \propto r^{-2.4}$. Fixing α, we re-fit the distribution of galaxy of clusters, extracting median values of $R_c = 0.05^{+0.02}_{-0.01}$ and $R_c/R_{virial} = 0.05$. Using all the aforementioned measurements and applying Eq. (7), we can calculate the virial masses of galaxy clusters using Eq. (3).

4. Results and discussions

In Tab. 1 we list the cluster parameters computed above: the name of sampled clusters (col. 1), the number of member galaxies N_m (col. 2) contained within the radius R (col. 5) and redshift (col. 3) with richness

Table 1: The optical masses and other parameters as compare with X-ray masses for 37 nearer Chandra galaxy clusters.

Name	N_m	z	rich	R_{max}, Mpc	σ_P, km s^{-1}	N	R_{vir}, Mpc	α^a	R^a_C, Mpc	R_{PV}, Mpc	M_{vir}, $10^{14}M_\odot$	M_X, $10^{14}M_\odot$
A2589	28	0.042	0	0.59	470±100	28	0.94	1.50	0.10	0.33±0.15	10.79±0.54	10.05±1.29
MKW4	51	0.019	1	3.58	525±75	42	1.05	1.10	0.07	0.47±0.06	1.42±0.43	2.22±2.10
AWM4	23	0.032	1	3.50	119±89	23	0.24	0.70	0.01	0.18±0.09	3.03±0.03	6.55±0.85
A2063	92	0.035	1	3.87	667±55	70	1.33	1.18	0.13	0.66±0.07	3.24±0.62	10.30±1.94
A576	199	0.038	1	1.74	914±55	199	1.83	1.03	0.25	1.22±0.15	17.15±1.84	21.11±2.16
A3376	75	0.046	1	2.29	688±68	65	1.38	0.62	0.01	0.89±0.07	24.63±0.99	26.61±3.72
A2717	55	0.049	1	1.16	541±65	54	1.08	0.76	0.08	0.80±0.09	12.57±0.68	12.94±2.11
A3391	50	0.051	1	0.87	663±195	50	1.33	0.73	0.06	0.92±0.15	14.45±2.72	18.91±1.28
A2124	61	0.065	1	1.22	878±90	61	1.76	1.50	0.30	0.88±0.15	7.40±1.98	13.12±1.37
A400	58	0.024	2	1.22	599±80	57	1.20	0.83	0.04	0.70±0.08	2.76±0.81	3.44±1.02
A262	82	0.017	2	3.95	525±47	40	1.05	0.59	0.01	0.87±0.13	2.64±0.60	2.93±0.73
A539	160	0.028	2	2.47	629±70	70	1.26	0.78	0.02	0.68±0.09	4.96±0.76	8.38±1.77
A2634	69	0.031	2	0.86	700±97	69	1.40	0.62	0.02	1.03±0.15	5.51±1.73	11.88±2.15
A3571	69	0.039	2	0.98	1045±109	69	2.09	1.23	0.14	0.73±0.15	18.69±2.55	30.41±3.84
A119	62	0.044	2	1.27	679±107	62	1.36	0.66	0.01	0.86±0.15	14.32±1.55	24.06±4.16
A1644	84	0.046	2	1.94	759±61	76	1.52	1.01	0.34	1.28±0.10	8.09±1.44	14.60±1.47
A3562	100	0.047	2	2.15	736±49	89	1.47	0.66	0.15	1.22±0.05	7.62±1.01	14.05±1.56
A754	77	0.054	2	2.60	662±77	62	1.32	1.50	0.31	0.98±0.08	34.71±1.16	40.30±3.71
A2256	86	0.058	2	1.19	1348±86	86	2.70	0.92	0.12	1.32±0.15	36.26±4.49	47.78±5.37
A3158	123	0.059	2	1.67	976±70	123	1.95	0.77	0.04	1.06±0.15	21.08±2.23	25.80±3.17
A1795	81	0.063	2	1.81	834±85	80	1.67	0.77	0.03	0.91±0.09	16.92±1.57	19.34±2.18
A399	79	0.071	2	1.56	1116±89	79	2.23	1.50	0.42	1.19±0.15	26.26±3.31	37.90±4.11
A401	106	0.074	2	2.00	1152±86	106	2.30	1.50	0.42	1.19±0.15	25.99±3.22	37.97±4.16
A2029	73	0.077	2	1.57	1164±98	73	2.33	1.10	0.05	0.48±0.15	17.19±2.54	33.43±4.12
A2142	86	0.091	2	1.63	1132±110	86	2.26	1.50	0.51	1.36±0.15	19.12±4.27	29.87±3.17
A3921	29	0.094	2	1.33	490±140	24	0.98	0.78	0.19	0.93±0.15	22.45±1.30	29.61±2.15
A1060	82	0.012	3	2.06	610±52	79	1.22	0.80	0.03	0.69±0.07	5.80±0.56	9.81±1.32
A2199	50	0.030	3	3.29	801±92	42	1.60	0.79	0.05	0.96±0.14	6.76±1.85	12.38±2.18
A496	55	0.033	3	1.10	687±89	55	1.37	1.50	0.27	0.76±0.15	5.91±1.27	9.10±1.27
MKW3s	30	0.045	3	3.47	610±69	27	1.22	0.75	0.01	0.59±0.15	12.40±0.81	12.02±3.19
A3395	99	0.050	3	1.14	852±84	99	1.70	1.50	0.25	0.76±0.15	26.05±1.68	33.67±4.27
A85	125	0.055	3	1.75	969±95	124	1.94	1.50	0.53	1.31±0.15	15.49±3.10	25.68±4.89
A3667	154	0.056	3	2.22	971±65	152	1.94	0.52	0.02	1.55±0.07	15.98±2.18	26.84±2.48
A3266	128	0.059	3	1.34	1107±82	128	2.21	0.64	0.19	1.91±0.15	25.67±4.31	33.25±4.16
A2670	197	0.076	4	2.22	852±50	186	1.70	0.93	0.12	0.99±0.06	7.89±1.02	16.62±1.62
Coma	283	0.023	5	3.90	821±50	171	1.64	0.79	0.09	1.08±0.07	37.98±1.09	41.94±4.72
A3558	341	0.048	5	1.99	977±40	338	1.95	0.85	0.18	1.25±0.05	13.10±1.16	21.27±3.27

(col. 4) and the global projected velocity dispersion σ_P with the respective errors (col. 6); the number of galaxies N (col. 7) within R_{virial} (col. 8); the values of α and R_c resulting from the fit to the galaxy distribution (cols. 9 and 10, respectively); the projected virial radius, R_{PV}, computed at P_{virial} (col. 11); the virial mass (col. 12) and the cluster's X-ray mass from Babyk et al. 2013a (col. 13). By applying σ_P and R_{PV}, we compute the virial mass M_{vir} within R_{virial} through the Eq. (3). We used the X-ray mass estimates for these clusters, which were obtained in our previous works (Babyk et al., 2012c; Babyk et al. 2013a) .

We found correlations between X-ray and optical mass. The masses of individual clusters do not extremely agree in several cases. Our estimates of virial masses is based on the assumption that mass follows the galaxy distribution, whereas X-ray masses do not require any assumption about the cluster mass distribution. This correlation between optical and X-ray masses shows a large scatter that cannot be explained by the observational errors (X-ray masses are systematically larger). The absence of trend in dependence of redshift is also in favor of a good quality observational data. The main discrepancies are related to the clusters of richness class 3 and suggest the presence of an intrinsic scatter, possibly due to some deviation from the "mass follows galaxies" law or from pure dynamical equilibrium (we did not analyze cluster substructures in detail).

Although our work is not devoted to the analysis of galaxy distribution, we have had to address this issue in the computation of cluster masses. In our previous works, the X-ray mass estimates (Babyk et al., 2013a) allowed to estimate a tight correlation between c_{200} and M_{200} , $c \propto M_{vir}/(1+z)^b$ with a = -0.56 ± 0.15 and b =0.80± 0.25 (95% confidence level). In addition, it was found that the inner slope of the density profile α correlates with the baryonic mass content M_b, namely: α is decreasing with increasing the baryonic mass content. Our previous calculations of physical parameters of intracluster gas in the wide redshift range was used then to obtain constraints on the "luminosity - temperature - mass of gas" relationship for the Chandra galaxy clusters at $0.4 < z < 1.4$ (Babyk et al., 2013b).

In this work using a King-like profile, we obtain good alternative estimates of individual virial radii (see Fig. 1), which we need in order to obtain reliable cluster mass estimates for the nearer clusters. Moreover, when one or two parameters (α, R_c) are fixed, the estimates of virial radii results are less good, supporting the existence of an intrinsic spread of cluster parameters. As for the comparison with previous King-like fits, we find good agreement with the value of the exponent α obtained by Girardi et al. (1995) ($\alpha = 0.8^{+0.3}_{-0.1}$). So, the agreement between optical and X-ray masses is well explained in the context of two common assumptions: that mass follows the galaxy distribution, and that about 70 % of studied nearer clusters are not far from dynamical equilibrium.

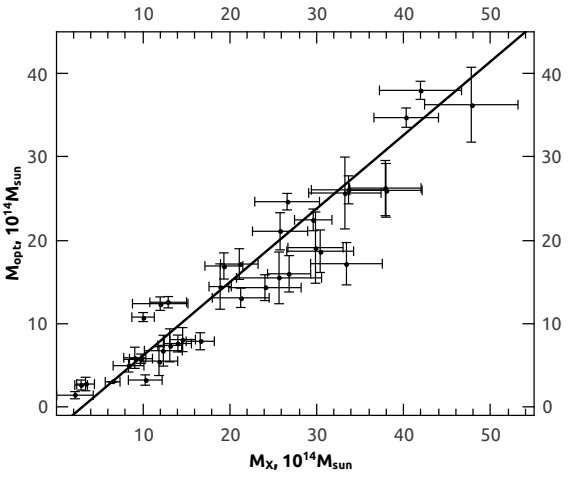

Figure 1: The correlation between optical and X-ray masses of clusters determined by different methods. The solid line corresponds the linear fit of sample.

Acknowledgements. This work was partially supported in frame of the Target Program of Space Scientific Research of the NAS of Ukraine (2012-2016).

References

Babyk Iu., Melnyk O., Elyiv A. et al.: 2012a, *Kinematics and Physics of Celestial Bodies*, **28**, p.69.

Babyk Iu.: 2012b, *Journal of physical studies*, **16**, p.7.

Babyk Iu., Vavilova I., Del Popolo A.: 2013a, *submitted to Astronomy Reports*, **arXiv:1208.2424**.

Babyk Iu., Vavilova I.: 2013b *Astrophys. and Space Sci.*, **DOI 10.1007/s10509-013-1630-z**.

Babyk Iu., Vavilova I.: 2012c, *Odessa Astronomical Publications*, **25**, p. 119.

Babyk Iu.: 2012d, *Izvestiya Krymskoi Astrofizicheskoi Observatorii*, **108**, p.127.

Choi Y., Han D., Kim S.: 2010, *JKAS*, **43**, p.191.

Fadda D., Girardi M., Giuricin G. et al.: 1996, *ApJ*, **473**, p.670.

Girardi M., Biviano A., Giuricin G. et al.: 1995, *ApJ*, **438**, p.527.

Girardi M., Borgani S., Giuricin G. et al.: 1998, *ApJ*, **506**, p.45.

Yang X., Mo H., van den Bosch F., Jing Y.: 2005, *MNRAS*, **356**, p.1293.

Yang X., Mo H., van den Bosch F. et al.: 2007, *ApJ*, **671**, p.153.